Magnetic Resonance Imaging, Vol. 6, pp. 125-130, 1988
Printed in the USA. All rights reserved.

0730-725X/88 $3.00 + .00

● *Original Contribution*

SAR REDUCED PULSE SEQUENCES

JAMIE E. HECKER PROST,* FELIX W. WEHRLI,* BURTON DRAYER,** JERRY FROELICH,† DAVID HEARSHEN,† AND DONALD PLEWES‡

*General Electric Co. (Medical Systems Group), Milwaukee, WI, **St. Joseph's Hospital, Phoenix, AZ, †Henry Ford Hospital, Detroit, MI, ‡Strong Memorial Hospital, Rochester, NY.

Three techniques were considered for reducing the RF (radiofrequency) power deposition in the body while maintaining scan time efficiency: reducing the RF peak amplitude while increasing the pulse width, substituting gradient echoes for spin echoes, and reducing the flip angle of the phase reversal pulse. The use of gradient echoes was found to be the most efficient means to reduce the power delivered to the patient and to obtain rapid data acquisition. The effect upon SAR (specific absorption rate) and SNR (signal-to-noise ratio) was demonstrated on a phantom when the phase reversal pulse was reduced from the standard 180° to 90°. Data in the body indicated a fairly constant SNR down to a refocusing flip angle between 110° and 135°. An initial clinical evaluation was performed at three institutions using the method of reducing the flip angle of the phase reversal pulse. The scan with $\theta = 120°$ was rated by readers in a blinded study as having acceptable diagnostic image quality while the 135° scan had comparable image quality to a conventional 90°-180° pulse sequence. The use of reduced phase reversal pulses was seen as an efficient protocol to obtain T_1-weighted images at rapid data rates while reducing the power delivered to the body by about 40%.

Keywords: **Magnetic resonance, Image quality, Physics.**

INTRODUCTION

The specific absorption rate (SAR) is defined as the rate of energy deposition caused by radiofrequency radiation in the human body. SAR is measured in Watts/kilogram (W/kg). Two figures are of relevance: the average SAR over the total body weight and the peak SAR, which is the maximum SAR over any one gram of tissue scanned.

The purpose of this study was to investigate whether it was possible to reduce RF power deposition in the body without sacrificing efficiency of scanning. It is important to note in this context that the Food and Drug Administration (FDA) is currently considering reclassifying MR to a class II device with possibly an increase in power deposition being permitted.[7]

The specific absorption rate is given by Eq. 1.

$$SAR_{AVE} = Power_{TOTAL}/(Volume * Density) \quad (1)$$

Most of the deposited power results from a magnetic interaction of the B_1 field with electric dipoles and monopoles (ions) in the body fluids. Eq. 2 implies that the average SAR (SAR_{AVE}) is proportional to the conductivity (σ), the square of the resonance frequency (ω^2), and the square of the mean amplitude of the B_1 field $(\bar{B}_1)^2$.

$$SAR_{AVE} \propto \sigma(\omega \bar{B}_1)^2 \quad (2)$$

Since the pulse flip angle is equal to the magnetogyric ratio (γ) multiplied by the time integral of B_1 (Eqs. 3 and 3a), it follows in Eq. 4 that SAR_{AVE} is proportional to the sum of the flip angles squared, divided by the repetition time (TR), where θ_1 and θ_2 are the 90° and 180° pulse flip angles and n is the number of echoes.

$$\theta = \gamma \int B_1(t)dt \quad (3)$$

RECEIVED 8/20/87; ACCEPTED 8/20/87.

Address correspondence and reprint requests to Felix W. Wehrli, Ph.D., General Electric Company, Medical Systems Group, Magnetic Resonance: W-809, 3200 N. Grandview Blvd., Waukesha, WI 53188.

$$\bar{B}_1 = \gamma \int_0^{\tau} B_1(t)dt/\tau \qquad (3a)$$

$$SAR_{AVE} \propto (\theta_1^2 + n\theta_2^2)/TR \qquad (4)$$

Equation 4 assumes all parameters which affect SAR, like the coil type, RF pulse widths, patient weight, peak RF amplitude, RF pulse shape, anatomical region, and field strength, have been held constant. It then follows from Eq. 4 that in a pulse sequence containing one 90° pulse and one 180° RF pulse, 20% of the deposited power arises from the single 90° pulse while 80% of the power is due to the 180° pulse. Figure 1 is a plot of average power dissipation levels which relate the average SAR to the weight of the patient being scanned; these SAR values are calculated values for each scan based on prior curve fits to experimental data (General Electric 1.5T SIGNA, Milwaukee, WI). Let us assume a single-echo, multislice sequence with seven slices, TR = 500 ms, and 20 ms echo in a quadrature drive body coil operating at 64 MHz. For this particular scan sequence (i.e., 14 echoes/second), the average SAR would exceed 0.4 W/kg for patients above 150 lb body weight. One possible, although undesirable, remedy is to reduce the duty cycle of the RF transmitter (i.e., to reduce the number of slices per unit time). This situation may be viewed in Fig. 2, which plots the calculated average SAR versus the number of slices for three representative patient weights for the same pulse sequence (i.e., TR = 500 ms).

METHODS

Several methods come to mind that could be used to reduce the whole body average SAR. These include: (1) decreasing the peak amplitude of the RF pulses while increasing their pulse widths, (2) substituting gradient-recalled echoes for 90°/180° RF spin echoes,[4,5,8] and (3) reducing the flip angle of the phase reversal pulse. While any of these would reduce the power delivered to the patient, there are trade-offs and limitations for each of these possible technical alternatives.

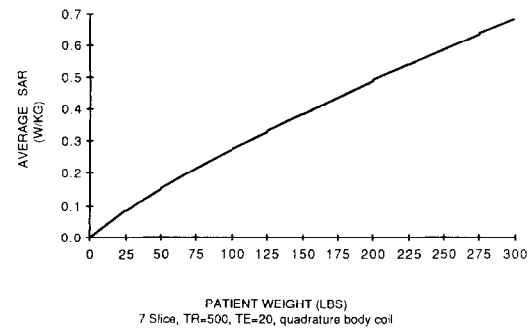

Fig. 1. Average SAR values for various patient weights for a seven-slice, single echo sequence in a TR of 500 ms with a quadrature body coil operating at 64 MHz.

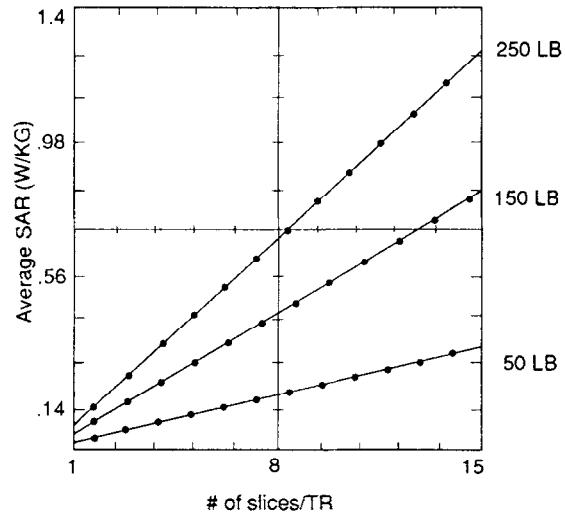

Fig. 2. Calculated average SAR values for a variable number of slices per TR (500 ms) at patient weights of 50, 150, and 250 lbs.

In (1), reducing the amplitude while increasing the width would result in an increase in the minimum echo time and would require an increase in the gradient strength to maintain the same slice thickness. The increased pulse width also makes the MR scan more sensitive to off-resonance effects because of the narrower bandwidth of the pulse. In (2), the gradient echo (or field echo) is sensitive to static field inhomogeneities and intrinsic gradients resulting from magnetic susceptibility variations.[3] The latter are well known to occur near air–tissue interfaces like sinus cavities, bowel, etc. In (3), reducing the flip angle of the phase reversal pulse results in some reduction in the signal-to-noise ratio and may be useful only for T_1-weighted images.

Among the three methods mentioned, the substitution of gradient echoes for RF echoes is by far the most efficient means to reduce the power delivered to the patient. This relationship is depicted in Fig. 3 of average SAR versus TR for flip angles of 10°, 30°, 50°, 70°, and 90°. These curves were calculated for a 250 lb patient assuming a single excitation per TR period. A typical setting for the flip angle is 30°. At the technical lower limit of TR (~20 ms) one would

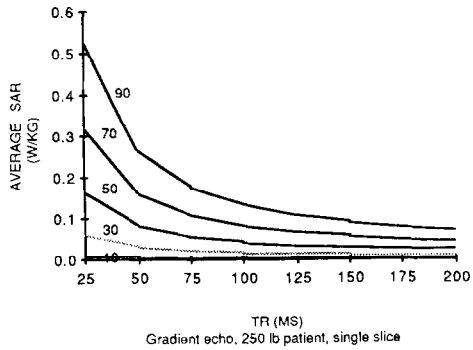

Fig. 3. Calculated average SAR values for various TRs assuming a gradient echo with flip angle of 10°, 30°, 50°, 70°, or 90° in a 250 lb patient.

therefore operate considerably below the 0.4 W/kg level.

This technique also allows very rapid image data acquisition. If we assume a total imaging time of 1 min with a 128 × 256 matrix and a single excitation per slice, current capabilities on the system allow for 27 slices using TR = 18 ms, as compared to 15 slices in an interleaved acquisition for the Carr-Purcell spin-echo with TR = 500 ms and TE = 20 ms. Figure 4 displays six out of seven GRASS (Gradient-Recalled Acquisition in the Steady-State)[10] abdominal images which were obtained with TR = 23.5 ms, TE (echo time) = 15 ms, θ = 15°, 10 mm slice thickness, 128 phase encodings, and NEX (number of excitations) = 1 in 25 sec. The average SAR value for this scan was less than 0.01 W/kg at a patient weight of 125 lbs.

Finally, we have investigated the third approach of reducing power deposition, i.e., lowering the flip angle of the phase reversal pulse. Instead of utilizing a 90°/180° RF pulse sequence, a 90°/θ RF pair is used with theta varied between 90° and 180°. In 1950, Hahn[9] demonstrated that any two RF pulses create a spectral distribution of magnetic moments which then precess to form a "spin-echo" (Hahn echo) in the transverse plane through constructive interference.[9] Since most of the RF power of the pulse sequence is in the 180° pulse, a reduction of the phase reversal pulse should, at the expense of some signal, result in less deposited power to the patient.

In the following experimental results, SNR was measured from regions of interest (ROI) as a function of the flip angle of the refocusing pulse. For this purpose, ROIs were placed within the object to provide a figure of merit for the mean signal intensity. Likewise, noise was determined from an ROI outside the object boundaries. The SNR is related to the signal

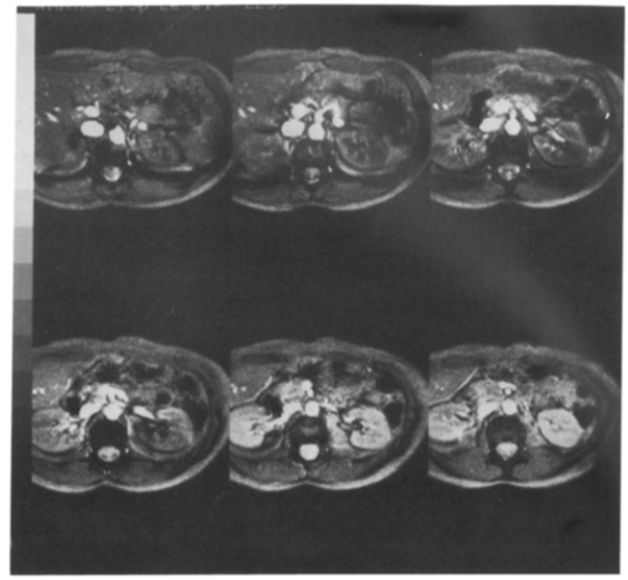

Fig. 4. GRASS images obtained in 25 sec at an average SAR level less than 0.01 W/kg.

amplitude, H, and true noise standard deviation, σ_t, as follows in Eq. 5 where n is the number of views, $\bar{p}$ is the mean signal intensity, and σ is the standard deviation within the ROI serving for the noise measurement. This formula for SNR compensates for the magnitude reconstruction used on the system.

$$\text{SNR} = \frac{H}{\sigma_t} = \frac{H}{\sqrt{\sigma^2 + \frac{n}{n-1}(\bar{p})^2}} \tag{5}$$

RESULTS

Figure 5 illustrates the effect upon average SAR values when the phase reversal pulse θ is gradually reduced from 180° to 90°. Three representative patient weights are depicted for a single echo sequence with TR = 500 ms and seven slices. In addition to the power reduction inherent to this method, there is a concomitant decrease in SNR due to the incomplete rephasing of the spins in the X-Y plane. This SNR dependence on θ is shown in Fig. 6, which plots the signal-to-noise value of a phantom consisting of CuSO4-doped water (0.01M) for various phase reversal pulses. The plotted SNR has been normalized to the value measured for the conventional 90°/180° pulse sequence. We note that the signal level remains at 90% of the maximum signal down to a θ = 130°, accompanied by a 40% reduction in SAR. For θ =

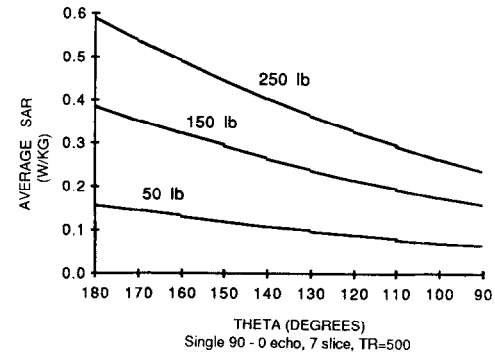

Fig. 5. Reduction in the average SAR has been achieved by gradually decreasing the phase reversal pulse flip angle from 180° to 90°.

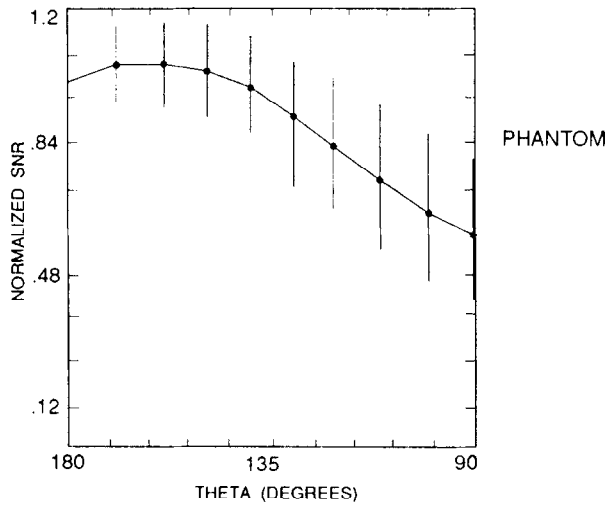

Fig. 6. SNR dependence on the slip angle of the refocusing pulse for the $CuSO_4$ phantom described in the text.

90°, SNR has dropped to 58% with an SAR reduction of 60%.

Surprisingly, the corresponding data obtained in humans are not in complete agreement with the phantom data. Measurements in the liver show an initial increase in SNR followed by a fairly flat region down to $\theta \sim 110°$. Data for Fig. 7 were acquired with a respiratory-compensated[1,6] multi-slice sequence with two excitations, six 10 mm slices, 256 × 256 matrix, TR = 600 ms and TE = 25 ms. Typical SNR values for liver and spleen were 22 and 27 for $\theta = 180°$ and 17 and 13 for $\theta = 90°$, respectively. As before, the SNR was normalized for the liver and spleen data in the 90°/180° scan. The relative insensitivity of liver SNR to the flip angle of the echo pulse may be an

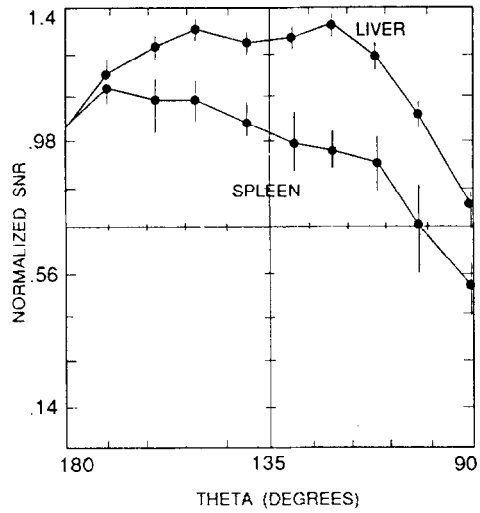

Fig. 7. Normalized SNR of liver and spleen for refocusing pulses varying between 180° and 90°. Note the relatively flat nature of the liver curve.

indication that the noise in the images is not dominated by either subject or electronics but perhaps may be influenced by the noise of the physiological motion. This explanation is supported by pelvic studies, where there is minimal physiological motion, which show fat and bone regions-of-interest having SNR fairly constant to $\theta = 135°$ and then slowly decreasing to ~50% SNR at $\theta = 90°$ (Fig. 8). ROIs at six slice locations were averaged for the liver SNR while 2 ROIs were averaged for the spleen data. The pelvic data represent an average of 6 ROIs for the bone and 7 ROIs for the fat tissue. The error bars on Figs. 6 through 8 indicate the mean standard deviation of the signal ROIs.

The method was subjected to clinical evaluation at three different institutions and found to be promising for rapid, T_1-weighted imaging. Figure 9 shows a leg fibrous histiocytoma with TR = 600 ms, TE = 25 ms, 32 cm field-of-view (FOV), 10 mm slice thickness, 128 × 256 matrix, and two excitations acquired in the body coil. The four images were obtained with refocusing pulses of 180°, 135°, 120°, and 90°, and are displayed with appropriate window and level settings. Although there is a perceptible loss of SNR in the 90°/90° image, the 90°/135° and 90°/180° scans are virtually indistinguishable. The pathology can clearly be visualized in all four images. The next case in Fig. 10 shows a cerebellar infarct displayed in the same format. A similar protocol was used for this scan except for a 5 mm slice thickness and 20 cm FOV in the head coil. Again, images obtained with 135° and

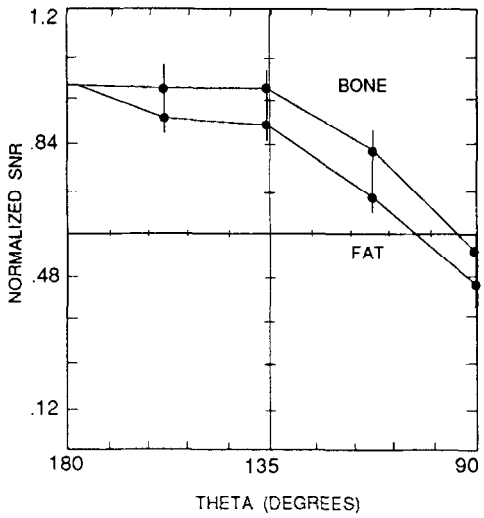

Fig. 8. Normalized SNR of fat and bone in the pelvis for refocusing pulses varying between 180° and 90°.

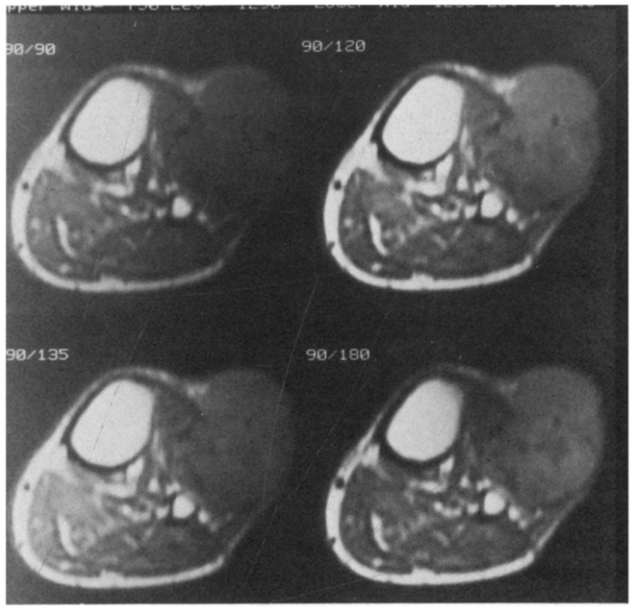

Fig. 9. Fibrous histiocytoma: The lesion is visualized in each of the images using (a) 90°, (b) 120°, (c) 135°, and (d) 180° refocusing pulse flip angles.

180° phase reversal pulses have comparable clinical utility with 35% less power deposition in the 135° scan. The final case is a lumbar spine with several punctate areas of high signal intensity which probably represent focal accumulations of fatty marrow (Fig. 11). The high signal intensity areas are still visualized in the 90°/90° RF acquisition. These images were

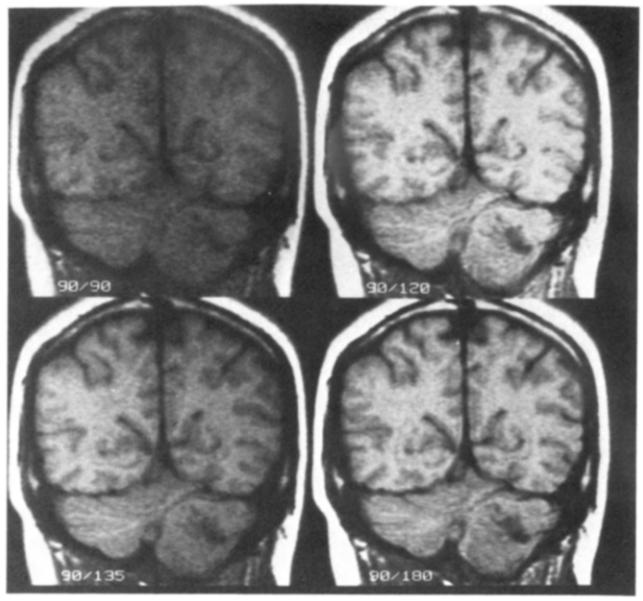

Fig. 10. Four acquisitions with various refocusing flip angles, (a) 90°/90°, (b) 90°/120°, (c) 90°/135°, and (d) 90°/180°, demonstrate cerebellar infarct.

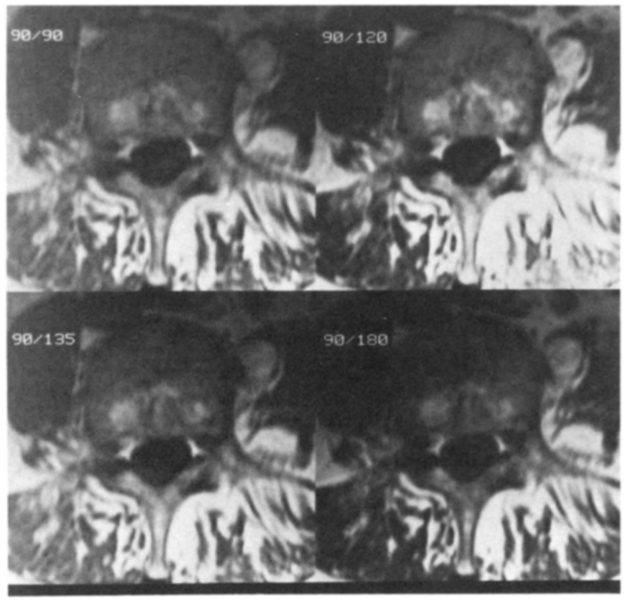

Fig. 11. Images of a patient with punctate areas of high signal intensity in the lumbar spine. The high signal intensity areas are visualized in all four scans using (a) 90°, (b) 120°, (c) 135°, and (d) 180° refocusing pulses.

obtained with a surface coil and TR = 600 ms, TE = 20 ms, four excitations, 5 mm slice thickness, 24 cm FOV, and 128 × 256 acquisition matrix. In a qualitative blind reading, four observers rated the surface

coil images of eight patients for overall image quality and visualization of the spinal cord, vertebral body, and disk. While the 90°/90° image was found to be of significantly lower quality, the 90°/120° scans were rated to be of acceptable quality and the 90°/135° scan of comparable quality to the standard 90°/180° acquisition.

DISCUSSION

In summary, the following conclusions may be made. The substitution of a gradient echo for RF is the most efficient method to reduce SAR. Reducing the flip angle of the phase reversal pulse is probably best for maintaining clinical SNR with a substantial power reduction. Although the $90°/\theta$ images have perceptibly reduced SNR for $\theta < 135°$, $\theta \geq 135°$ afforded images of comparable clinical utility. The use of a 120°–135° phase reversal pulse will result in a 45%– 35% power reduction which, under current regulations (SAR $\leq$ 0.4 W/kg), may be desirable for improving scanning efficiency in heavy patients. Although this method may be an efficient protocol to generate T_1-weighted images for screening large tissue volumes in the abdomen at data rates up to 30 slices per second, more work needs to be carried out to understand the clinical trade-offs. However, the proposed increase in allowable power deposition may make the investigation academic.[7]

REFERENCES

1. Bailes, D.R.; Gilderdale, D.J.; Bydder, G.M.; et al. Respiratory Ordered Phase Encoding (ROPE): A method for reducing respiratory motion artifacts in MR imaging. *J. Comp. Ass. Tom.* 9:835–838; 1985.
2. Bottomley, P.A.; Edelstein, W.A. Power deposition in whole-body NMR imaging. *Med. Phys.* 8(4):510–512; 1981.
3. Cox, I.J.; Bydder, G.M.; Gadian, D.G.; Young, I.R.; Proctor, E.; Williams, S.R.; Hart, I. The effect of magnetic susceptibility variations in NMR imaging and NMR spectroscopy in vivo. *J. Mag. Res.* 70:163–168; 1986.
4. Edelman, R.R.; Hahn, P.F.; Buxton, R.; Wittenberg, J.; Ferrucci, J.T.; Saini, S.; Brady T. Rapid MR imaging with suspended respiration: Clinical applications in the liver. *Radiology* 161:125–131; 1986.
5. Frahm, J.; Haase, A.; Matthaei, D. Rapid NMR imaging of dynamic processes using the FLASH technique. *Mag. Res. Med.* 3:321–327; 1986.
6. Glover, G.; Pelc, N. Control of ghost artifacts due to periodic subject motion in FT MR imaging. GE Medical Systems Group, Applied Science Laboratory Technical Note 84-61; 1984.
7. The Gray sheet. *Medical Devices, Diagnostics & Instrumentation Reports* 12(11):11; 1986.
8. Haase, A.; Frahm, J.; Matthaei, D.; Hanicke, W.; Merboldt, K.D. FLASH imaging: Rapid NMR imaging using low flip angle pulses. *J. Mag. Res.* 67:258–266; 1986.
9. Hahn, E.L. Spin echoes. *Phys. Rev.* 80:580–594; 1950.
10. Wehrli, F. Introduction to fast-scan magnetic resonance. General Electric Medical Systems Group, Publication No. 7299; 1986.